12th International Workshop on Innovative Simulation for Healthcare
20th International Multidisciplinary Modeling & Simulation Multiconference

2724-0045 © 2023 The Authors.
doi: 10.46354/i3m.2023.iwish.007

Newtonian and non-Newtonian blood model, a comparative study on large and small vessels

Gionata Fragomeni[1,*]

[1]Magna Graecia University, Catanzaro, 88100, Italy

[*]Corresponding author. Email address: fragomeni@unicz.it

Abstract

Newtonian fluid model has been commonly applied in simulating blood flow through vessels using Computational Fluid Dynamics (CFD) models, while blood is a non-Newtonian fluid. This work aimed to investigate the differences in CFD models built with Newtonian and non-Newtonian fluid assumptions. Two models were made (large and small vases). Static simulations on these models with Newtonian and two non-Newtonian (Carreau-Yasuda) fluid models were performed. Velocity, flow and Wall Shear Stress (WSS) values were evaluated in all CFD models. In all the simulations, we compared the hemodynamics values in CFD models derived with Newtonian and Carreau-Yasuda fluid assumptions. In all simulations, the Newtonian/non-Newtonian difference was negligible also for small and large vessels models.

Keywords: CFD; Newtonian flow; blood

1. Introduction

In recent years, computational fluid dynamics (CFD) modeling based on conventional vascular imaging has been applied to simulate blood flow and quantify hemodynamic parameters in the presence of various pathologies.

In most previous CFD studies, for simplicity blood was simulated as a Newtonian fluid, despite the fact that blood is a non-Newtonian fluid [Nader et al. 2019; Vinoth et al. 2017]. As flow velocity and shear strain rate increase, blood flows more smoothly [Moon et al., 2014, Johnston et al. 2006] and its viscosity decreases. However, in low-speed areas, the real viscosity is much higher than assumed, and non-Newtonian models could simulate changes in blood viscosity in these areas. Previous studies simulating blood flow in intracranial aneurysms, normal aorta and arterial stenosis models indicated differences in pressure and Wall Shear Stress (WSS) estimates based on Newtonian and non-Newtonian models [Hippelheuser et al., 2014; Rabby et al., 2014; Husain et al. 2012].

In this study, we therefore aimed to investigate the differences, if any, of the CFD simulation results in Newtonian and non-Newtonian fluid models, in large and small vessels; static simulations were performed on patient-specific geometric models.

2. Materials and Methods

Models of small (coronary) arteries (fig. 1-a) and one large artery (aorta) (fig. 1-b) were analyzed.

3D patient-specific coronary artery geometries were obtained from a series of angiograms acquired during a

standard x-ray angiography due to clinical reasons.

Aorta geometry was reconstructed starting from a series of slices, which were acquired *in-vivo* through the computer tomography (CT). This patient-specific aorta morphology was obtained using Itk-Snap, an open-source segmentation software (www.itksnap.org/). Since it provides a stereolithographic file (stl format), the 3D aorta with faceted surfaces was converted in a 3D solid model by means of the reverse engineering process. The aorta model included the ascending aorta, the aortic arch with its three epiaortic vessels (brachiocephalic artery, left carotid artery, left subclavian artery) and the descending aorta with the thoracic branches (Figure 1).

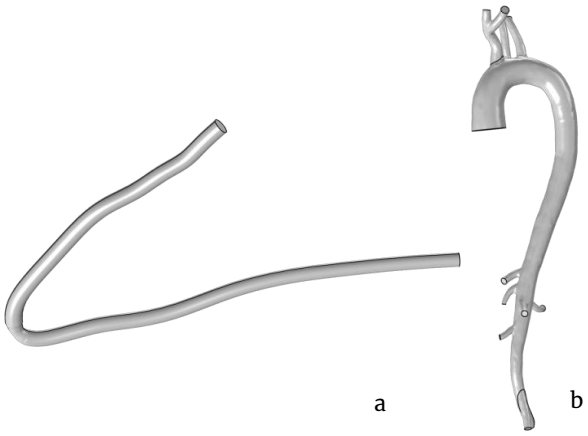

Figure 1. Coronary and Aorta Geometrical models

Static CFD simulations were performed separately with Newtonian and non-Newtonian fluid models (Casson and Carreau-Yasuda).

Blood viscosity in the Newtonian model was a constant: $\eta = 0.0035 Pa \cdot s$. The Carreau-Yasuda model is a common non-Newtonian blood model.

For the Newtonian model, 3D Navier-Stokes equations were used as governing laws [Gramigna et al. 2015].

The incompressible condition gives:

$$\nabla . u = 0 \qquad (1)$$

The governing equation used to solve the laminar model is:

$$\rho \frac{\delta u}{\delta t} + \rho(u.\nabla)\mathrm{u} = \nabla.\{-pI + \mu[\nabla \mathrm{u} + (\nabla \mathrm{u})^T]\} \qquad (2)$$

where ρ is the fluid density, u is the fluid velocity, p is the pressure, I is the unit diagonal matrix and μ is the viscosity [Gramigna et al. 2015].

The Carreau model is used with the viscosity-shear rate relation:

$$\eta = \eta_\infty + (\eta_0 - \eta_\infty)[1 + (\lambda\gamma)^2]^{\frac{n-1}{2}} \qquad (3)$$

where $\eta_0 = 0.056\ [Pa\ s]$ is the zero shear rate viscosity, $\eta_\infty = 0.0035\ [Pa\ s]$ is the infinite shear rate viscosity, $\lambda = 3.313\ [s]$ is a parameter, and $n = 0.3568$ is a dimensionless parameter [20]. The blood density ρ is assumed equal to 1060 $[Kg/m3]$ [Caruso et al. 2015].

The flow pattern analysis is described using Reynolds number (Re) [Formaggia et al. 2010], which compares the inertial force to the viscous force, as indicated below:

$$Re = \frac{\rho * \upsilon * D}{\mu} \qquad (4)$$

where ρ is the fluid density, υ is the average velocity, D is the hydraulic diameter, and μ is the dynamic viscosity [Formaggia et al. 2010]. *Re* was calculated for eleven artery coronary geometries of different patients, with a flow waveform inlet boundary condition and patient-specific pressure outlet boundary condition.

The boundary conditions of CFD domain were allocated on the basis of vessel sizes at each inlet and outlet, a steady-state simulation was performed and the peak velocity was assumed as an inlet boundary condition for all simulations, considering a fully developed profile [Caruso et al. 2015, Sohns et al. 2015].

As an outlet condition, a specific pressure was applied for each case.

The Computational Fluid Dynamics simulations were done using COMSOL Multiphysics 6.0 (Burlington, MA, USA). The meshes had boundary layers and tetrahedral and triangular elements, according to the geometry optimized by analyzing the error trend as a function of simulation time.

3. Results and Discussion

From the results of the simulations carried out, there are no particular differences between the two models used, especially for the speeds (figure 2). Figure 2 shows only the results of the Newtonian model, as those of the non-Newtonian model are completely superimposable. A check was carried out on the flow rates in the various branches and the differences are completely negligible.

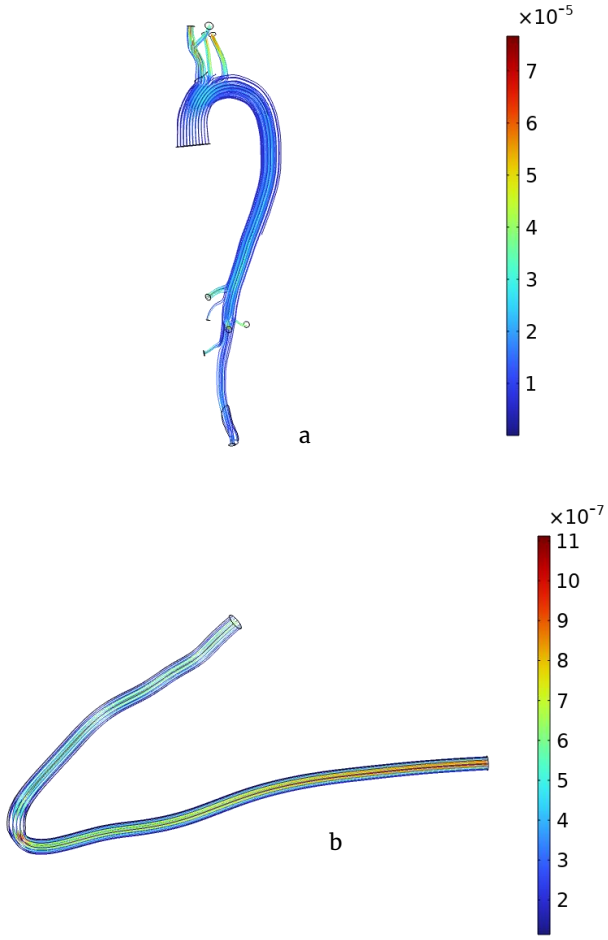

Figure 2. Aorta and coronary streamlines [m/s] for the Newtonian model.

On the other hand, as far as the WSS is concerned, there is a small difference between the two models, and the difference increases as the section of the vessel varies (Figure 3).

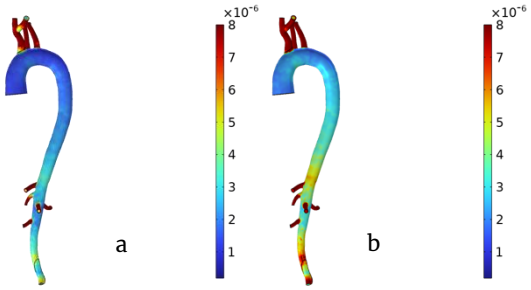

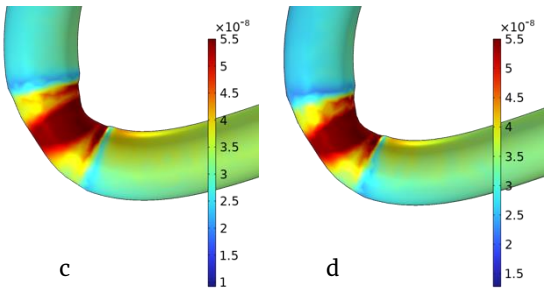

Figure 3. Aorta and coronary WSS [Pa] for the Newtonian model (a and c) and for the non-Newtonian model (b and d).

4. Conclusions

This study indicates that there is a negligible difference between CFD models with Newtonian and non-Newtonian fluid assumptions. As for the WSS results, the difference between Newtonian and non-Newtonian models is minimal in the high WSS area but slightly greater in the low WSS area. Therefore, the Newtonian fluid assumption might be applied in estimating WSS in high WSS regions, but caution should be exercised when using the Newtonian assumption in estimating WSS in low WSS regions.

References

Caruso M.V., De Rosa S., Indolfi C., Fragomeni G. Computational analysis of stenosis geometry effects on right coronary hemodynamics. In Engineering in Medicine and Biology Society (EMBC), 2015 37th Annual International Conference of the IEEE (pp. 981-984). IEEE. 2015. doi: 10.1109/EMBC.2015.7318528

Formaggia L, Quarteroni A. (Eds.). Cardiovascular Mathematics: Modeling and simulation of the circulatory system (Vol. 1). Springer Science & Business Media. 2010.

Gramigna, V., Caruso, M. V., Rossi, M., Serraino, G. F., Renzulli, A., & Fragomeni, G. (2015). A numerical analysis of the aortic blood flow pattern during pulsed cardiopulmonary bypass. Computer methods in biomechanics and biomedical engineering, 18(14), 1574-1581.

Iqbal Husain, Fotini Labropulu, Chris Langdon and Justin Schwark A comparison of Newtonian and non-Newtonian models for pulsatile blood flow simulations J Mech Behav Mater 2012; 21(5-6): 147–153

Barbara M. Johnston, Peter R. Johnston, Stuart Corney, David Kilpatrick, Non-Newtonian blood flow in human right coronary arteries: Transient simulations, Journal of Biomechanics, Volume 39, Issue 6, 2006, Pages 1116-1128, ISSN 0021-9290, https://doi.org/10.1016/j.jbiomech.2005.01.034.

Liu H, Lan L, Abrigo J, Ip HL, Soo Y, Zheng D, Wong KS,

Wang D, Shi L, Leung TW and Leng X (2021) Comparison of Newtonian and Non-newtonian Fluid Models in Blood Flow Simulation in Patients With Intracranial Arterial Stenosis. Front. Physiol. 12:718540. doi: 10.3389/fphys.2021.718540

Hippelheuser, J. E., Lauric, A., Cohen, A. D., and Malek, A. M. (2014). Realistic non-Newtonian viscosity modelling highlights hemodynamic differences between intracranial aneurysms with and without surface blebs. J. Biomech. 47, 3695–3703. doi: 10.1016/j.jbiomech.2014.09.027

Nader, E., Skinner, S., Romana, M., Fort, R., Lemonne, N., Guillot, N., et al. (2019). Blood Rheology: key parameters, impact on blood flow, role in sickle cell disease and effects of exercise. Front. Physiol. 10:1329. doi: 10.3389/fphys.2019.01329

Sohns, J., Kowallick, J., Joseph, A., Merboldt, K., Voit, D., Fasshauer, M., Staab, W., Frahm, J., Lotz, J., & Unterberg-Buchwald, C. (2015). Peak flow velocities in the ascending aorta—real-time phasecontrast magnetic resonance imaging vs. cine magnetic resonance imaging and echocardiography. Quantitative Imaging In Medicine And Surgery, 5(5), 685-690. doi:10.3978/j.issn.2223-4292.2015.08.08

Rabby, M. G., Shupti, S. P., and Molla, M. M. (2014). Pulsatile non-Newtonian laminar blood flows through arterial double stenoses. J. Fluids 2014, 1–13. doi: 10.1155/2014/757902

Vinoth R, Kumar D, Raviraj Adhikari and Vijay Shankar CS Non-Newtonian and Newtonian blood flow in human aorta: A transient analysis Biomedical Research (2017) Volume 28, Issue 7